Available online at www.sciencedirect.com
SCIENCE DIRECT®
Journal of Organometallic Chemistry 689 (2004) 2236–2241
Journal of Organometallic Chemistry
www.elsevier.com/locate/jorganchem

Alkyl group dependence of C–Si reductive eliminations from alkyl(silyl) Pt(II) complexes: a density functional study

Hideo Sakurai, Manabu Sugimoto *

Division of Molecular Engineering, Graduate School of Science and Technology, Satellite Venture Business Laboratory, Kumamoto University, Kurokami 2-39-1, Kumamoto 860-8555, Japan

Received 10 March 2004; accepted 8 April 2004

Abstract

C–Si reductive elimination from $Pt(R)(SiPh_3)(PMe_3)_2$ (R = Me, Pr) was theoretically studied with the density functional theory. For comparisons with the experiment, substitution of PMe_3 with diphenylacetylene was taken into account. The calculated activation barriers in the C–Si elimination step after the ligand exchange were 22.0 and 28.9 kcal mol^{-1} for R = Me and Pr, respectively, which explains the reactivity difference reported experimentally. In order to analyze the energy difference, we optimized transition states of several model complexes, and examined the influence of the steric repulsion between R and the other ligands. Comparisons of the geometries and the barrier heights reveal that the steric repulsion and the Si–alkyl bond energy are important factors controlling the reaction rate.

Keywords: DFT calculations; C–Si reductive elimination; Alkyl(silyl) Pt complex; Steric repulsion

1. Introduction

Reductive elimination of the C–Si bond is a product-forming process in hydrosilylation of unsaturated hydrocarbons catalyzed by transition metal complexes [1]. Detailed studies on this process are still limited [2–7] in spite that hydrosilylation is one of the important synthetic reactions for organosilyl compounds. This is probably because a reactant of this elementary process corresponds to an unstable intermediate which is difficult to be identified.

Systematic experimental studies on the reductive elimination have been carried out by Ozawa et al. [2,3] who synthesized comparatively stable alkyl(silyl)platinum complexes such as $Pt(Me)(SiPh_3)(PMePh_2)_2$. By measuring reaction rates of C–Si reductive eliminations from these complexes, they found that the reaction was very slow in pure solvent, and addition of electron-withdrawing alkyne (PhC≡CPh) effectively promoted the reaction. Their observations imply that a PMe_3–(PhC≡CPh) ligand exchange enhances the reactivity in the C–Si elimination. This is supported by the ab initio calculations [4] indicating that the activation barrier of the C–Si elimination from $Pt(Me)(SiH_3)(PH_3)_2$ is 24.3 kcal mol^{-1}, while it is 13.2 kcal mol^{-1} for $Pt(Me)(SiH_3)(PH_3)$ ($H_2C{=}CH_2$). The lowering of the activation barrier was ascribed to attractive back-donating interaction between ethylene π^* and Pt d orbital.

Ozawa and co-workers [5] also compared reaction rates of C–Si reductive eliminations from $Pt(R)(SiPh_3)(PMe_2Ph)_2$ complexes where R = Me, Et, Pr, and Bu. For R = Et, Pr, and Bu, the reaction rates (k) were shown much smaller than R = Me: $k = 33 \times 10^{-4}$ (R = Me) $> 2.5 \times 10^{-4}$ (Et) $> 1.6 \times 10^{-4}$ (Pr) $> 1.4 \times 10^{-4}$ (Bu) s^{-1} at 55 °C in solution. The reactivity difference is due to the fact that a rate constant in the direct C–Si reductive elimination remarkably depends on the alkyl group: $k = 33 \times 10^{-4}$ (R = Me) $> 1.0 \times 10^{-4}$ (Et) $> 0.61 \times 10^{-4}$ (Pr) $> 0.58 \times 10^{-4}$ (Bu) s^{-1} [5]. It was pointed out that, since the transition state is product-like, the activation energy mainly reflects the Si–alkyl bond energy. Another possible explanation would be that bulkiness of

* Corresponding author. Tel./fax: +81-96-342-3650.
E-mail address: sugimoto@kumamoto-u.ac.jp (M. Sugimoto).

0022-328X/$ - see front matter © 2004 Elsevier B.V. All rights reserved.
doi:10.1016/j.jorganchem.2004.04.014

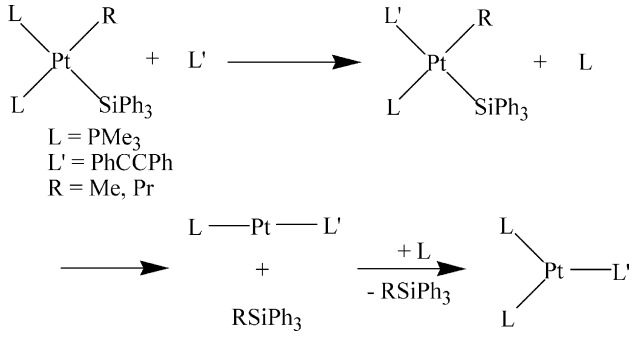

Scheme 1.

the alkyl group controls the barrier height. In the present paper, we report electronic structure calculations on the direct C–Si reductive elimination (Scheme 1) from $Pt(R)(SiPh_3)(PMe_3)(PhC{\equiv}CPh)$ with a particular interest on steric effects due to the alkyl group.

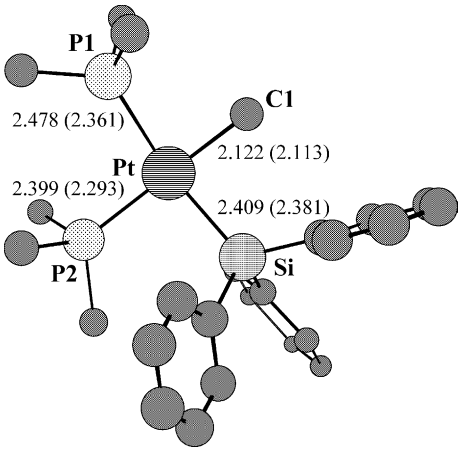

Fig. 1. Optimized geometry of $Pt(Me)(SiPh_3)(PMe_3)_2$. H atoms are omitted for clarity. The Pt–ligand distances are given in Å. Values in parentheses are those measured in the X-ray diffraction analysis for $Pt(Me)(SiPh_3)(PMePh_2)_2$ ([3]).

2. Computational details

Geometries of molecules in Scheme 1 and transition states were optimized by using the hybrid density functional theory (DFT) with the B3LYP functional [8]. Vibrational frequencies were calculated in order to confirm the nature of the stationary points. The core electrons of Pt (up to 4f) and P (up to 2p) were replaced by Hay and Wadt's [9] effective core potentials, and the outer electrons of the Pt and P atoms were represented with the (5s6p3d)/[3s3p2d] and (3s3p)/[2s2p] basis sets, respectively. For C and Si atoms, the 6-31G basis sets were employed [10], and the (31) set was used for H [11]. We added polarization d functions with exponents equal to 0.80 and 0.45 on eliminating C (connected to Pt) and Si atoms, respectively. The diffuse p (exponent: 0.0289) and polarization d (exponent: 0.364) functions were added to the P atoms. Zero-point energy (ZPE) corrections were made in evaluating reaction energies. These calculations were performed with GAUSSIAN 98 [12].

3. Results and discussion

3.1. Accuracy of the geometry optimization

In Fig. 1, the optimized geometry of the starting complex, $Pt(Me)(SiPh_3)(PMe_3)_2$, is shown and compared with the experimental one for $Pt(Me)(SiPh_3)(PMePh_2)_2$ [3]. The former Pt complex takes a square–planar structure, and the sum of the four angles around the Pt atom is calculated to be 360.7°: Si–Pt–C1 = 85.0°, P1–Pt–P = 96.5°, P1–Pt–C1 = 84.8°, P2–Pt–Si = 94.4°. These are in agreement with the experimental values of 82.2°, 98.0°, 85.2°, and 94.5°, respectively. The calculated Pt–C and Pt–Si distances also agree well with the corresponding experimental values. The two Pt–P distances are somewhat overestimated in the present calculation, although the d-polarization functions on the P atoms were included. In order to estimate a numerical error due to the calculated longer Pt–P bonds, we performed geometry optimization for $Pt(Me)(SiPh_3)(PMe_3)_2$ with the fixed Pt–P distances equal to the experimental values (2.361 and 2.293 Å). The energy deviation was calculated to be +2.0 kcal mol^{-1}. This small energy difference would be canceled out because the phosphine ligand plays a minor role on the reaction coordinate. Thus it is reasonably expected that relative energies of the stationary points discussed below would be rather insensitive to the Pt–P bond.

3.2. PMe_3–(PhC≡CPh) ligand exchange step

Experimentally, it was shown that an excess amount of PhC≡CPh promoted the C–Si reductive elimination

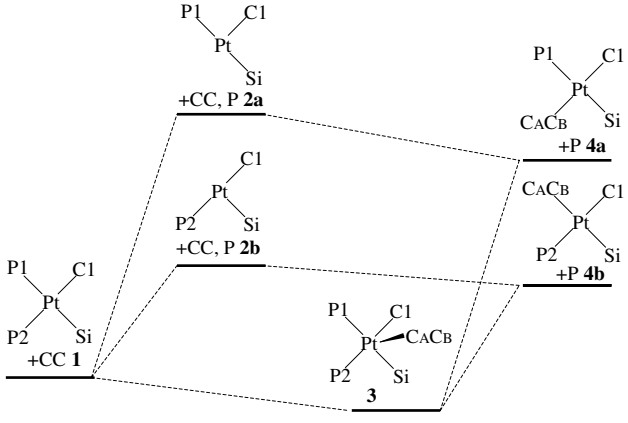

Scheme 2.

Table 1
B3LYP optimized geometries and relative energies of the alkyl(silyl) Pt complexes in Scheme 2

	Internuclear distance (Å)						E (kcal mol^{-1})
	Pt–P1	Pt–P2	Pt–C1	Pt–Si	Pt–CA	Pt–CB	
R = Me							
1	2.478	2.399	2.122	2.409			0.0
2a	2.473		2.051	2.339			23.6
2b		2.397	2.063	2.322			12.2
3	2.478	2.396	2.122	2.408	6.325	6.325	−1.2
4a	2.532		2.090	2.399	2.307	2.312	14.4
4b		2.405	2.071	2.321	4.007	4.029	9.6
R = Pr							
1	2.493	2.419	2.132	2.412			0.0
2a	2.479		2.064	2.354			20.4
2b		2.407	2.073	2.322			10.8
3	2.489	2.430	2.129	2.415	5.948	6.306	−1.2
4a	2.558		2.103	2.395	2.310	2.343	14.1
4b		2.418	2.077	2.322	4.264	4.302	8.8

from $Pt(R)(SiPh_3)(PMe_2\ Ph)_2$. This implies a possibility that the PMe_3–(PhC≡CPh) ligand exchange would be dependent on the alkyl group. Thus we here examine the ligand exchange step.

Scheme 2 presents two possible reaction routes of the ligand displacement step. One is a dissociative mechanism where PMe_3 elimination is followed by PhC≡CPh coordination (**1** → **2a**, **2b** → **4a**, **4b**). Another is an associative one where PhC≡CPh coordination is followed by PMe_3 elimination (**1** → **3** → **4a**, **4b**). Table 1 summarizes geometrical parameters and relative energies of the stationary points. The PMe_3-eliminated complex, $Pt(R)(SiPh_3)(PMe_3)$, is considered in the dissociative mechanism. The P1 elimination (*trans* to $SiPh_3$) yields **2b** with destabilization energies of 12.2 and 10.8 kcal mol^{-1} for R = Me and Pr, respectively. The P2 elimination complexes (**2a**) for R = Me and Pr are calculated to be 11.4 (R = Me) and 9.6 (R = Pr) kcal mol^{-1} higher than **2b**, indicating that formation of **2a** is energetically unfavorable. In the association mechanism, PhC≡CPh coordination yields $Pt(R)(SiPh_3)(PMe_3)_2$ (PhC≡ CPh) (**3**) with stabilization energy of 1.2 kcal mol^{-1} for both R = Me and Pr. For **3**, P1 elimination yields a ligand-displaced complex (**4b**) with destabilization energies of 10.8 (R = Me) and 10.0 (R = Pr) kcal mol^{-1}. The P2 elimination complex (**4a**) is 4.8 (R = Me) and 5.3 (R = Pr) kcal mol^{-1} higher than **4b**.

In the dissociative mechanism, the P1 elimination complex (**2b**) with R = Me (Pr) is only 2.6 (2.0) kcal mol^{-1} less stable than **4b**. This small energy difference indicates that both dissociative (**1** → **2b** → **4b**) and associative (**1** → **3** → **4b**) mechanisms would similarly contribute to the ligand displacement. The relative energies of the stationary points along each reaction path are little dependent on the alkyl group (R) within the tolerance of 1.4 kcal mol^{-1}. Therefore, it is concluded that the alkyl-group dependence does not appear in the ligand exchange step.

3.3. C–Si reductive elimination step

Fig. 2 shows relative energies of the stationary points in the C–Si reductive elimination from **4b**. Activation energies of this process for R = Me and Pr were calculated to be 22.0 and 28.9 kcal mol^{-1}, respectively. These are larger than the reaction energies required in the PMe_3–(PhC≡CPh) ligand exchange step, indicating that this C–Si elimination step is rate-limiting. The activation energy of the Pr complex is calculated to be 6.9 kcal mol^{-1} higher than that of the Me complex, which is consistent with the experimentally observed reactivity order (Me > Pr). The optimized transition state geometries are shown in Fig. 3. It is found that the Pt–C1 distance of the Pr complex is 0.261 Å longer than that of the Me complex. These transition states are non-planar. The dihedral angles (δ) between the Pt–P–X (X: midpoint of C≡C) and Pt–Si–C1 planes in Fig. 3 indicate that the TS geometries for R = Me and Pr are distorted

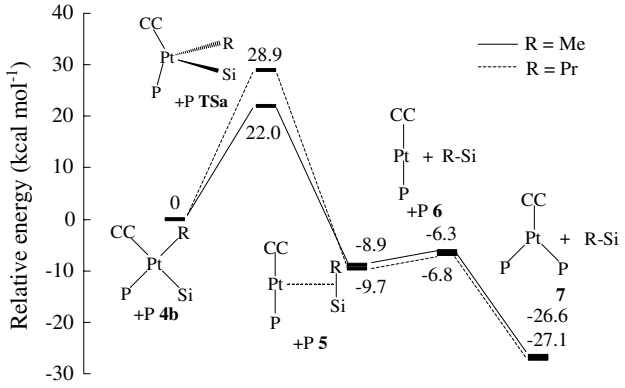

Fig. 2. Relative energies of the stationary points in the C–Si elimination step. CC, P, and Si indicate PhC≡CPh, PMe_3, and $SiPh_3$, respectively.

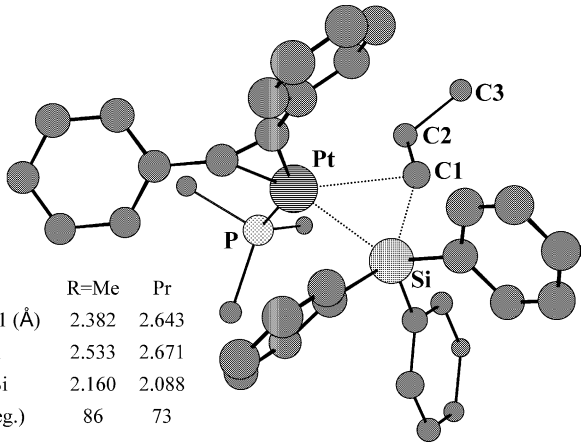

	R=Me	Pr
Pt-C1 (Å)	2.382	2.643
Pt-Si	2.533	2.671
C1-Si	2.160	2.088
δ (deg.)	86	73

Fig. 3. Optimized transition-state geometry of $Pt(R)(SiPh_3)(PMe_3)(PhC{\equiv}CPh)$ (R = Pr). For R = Me, some selected parameters are compared.

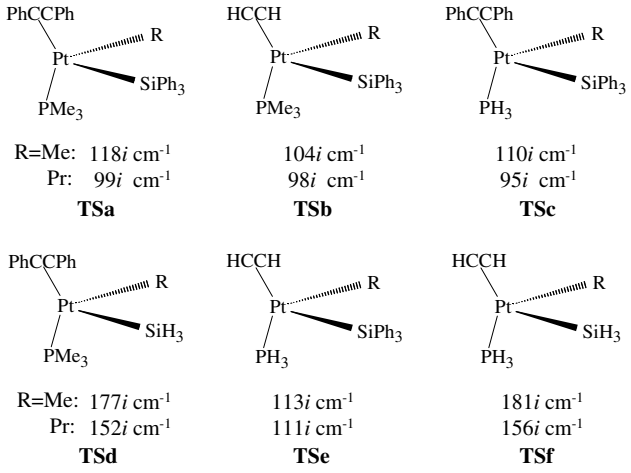

Fig. 4. Model complexes for the analysis of the transition state in the C–Si reductive elimination. The imaginary frequencies calculated in the normal mode analysis are also shown.

similar to the one previously reported for $Pt(PH_3)_2(CH_3)(SiH_3)$ [13]. The distortion was ascribed to steric repulsion between the CH_3–SiH_3 and PH_3 groups.

In order to clarify the origin of the R dependence of the activation energy, we examined transition states of five model compounds (**TSb**–**TSf**) in Fig. 4. Table 2 summarizes bond distances in the optimized geometries and activation energies. The Pt–C1 internuclear distance (see also Fig. 3) for R = Me changes within 0.048 Å, while it does within 0.234 Å for R = Pr. Changes in the Pt–Si (within 0.237 Å) and Si–C1 (0.081 Å) distances are also appreciable in the Pr complexes. Thus, geometry of a Pr complex is sensitive to a ligand substitution considered in Fig. 4. When $SiPh_3$ is coordinated (**TSa**–**TSc**, **TSe**), the Si–C2 and Si–C3 internuclear distances in the Pr complex become longer. This means that the propyl group changes its orientation in the $SiPh_3$ complex. Therefore, it is considered that steric effect plays an important role in Pr complex.

Importance of the steric repulsion can also be confirmed by model calculations where **TSa** and **TSd** are re-optimized with a fixed dihedral angle (θ) between the Pt–Si–C1 and Pt–C1–C2 planes (Table 3). This dihedral angle controls a distance between the silyl group and the ethyl moiety of the propyl ligand. In the fully optimized **TSa** and **TSd**, θ are 148° and 106°, respectively. When θ is decreased, the Et–silyl distance becomes small, which reinforces the steric repulsion. Table 3 shows that the Si–C1 bond distances slightly elongated (+0.059 and +0.077 Å for **TSa** and **TSd**, respectively) when the repulsion between the Et and silyl moieties is enhanced ($\theta = 106°$). On the other hand, Pt–C1 internuclear distances decrease in 0.154 and 0.204 Å for **TSa** and **TSd**. This decrease can be attributed to reduction of steric repulsion between Pr and $Pt(PMe_3)$ moieties. The

Table 2
B3LYP-optimized geometrical parameters and activation energies (without ZPE) of the transition states shown in Fig. 4

	Internuclear distance (Å)					E_{act} (kcal mol^{-1})
	Pt–C1	Pt–Si	Si–C1	Si–C2	Si–C3	
R = Me						
TSa	2.382	2.533	2.160			21.6
TSb	2.422	2.581	2.105			17.6
TSc	2.388	2.562	2.133			19.8
TSd	2.396	2.442	2.139			15.1
TSe	2.389	2.570	2.128			17.7
TSf	2.374	2.459	2.140			12.9
R = Pr						
TSa	2.642	2.671	2.088	3.430	4.583	28.5
TSb	2.616	2.675	2.099	3.439	4.588	24.9
TSc	2.526	2.712	2.102	3.340	4.486	24.7
TSd	2.469	2.475	2.126	3.113	4.375	17.0
TSe	2.408	2.574	2.169	3.205	4.382	20.7
TSf	2.435	2.481	2.132	3.118	4.381	14.0

Table 3
Bond distances in **TSa** and **TSd** optimized with a fixed dihedral angle (θ) between the Pt–Si–C1 and Pt–C1–C2 planes

	$\theta = 106°$	$\theta = 148°$
TSa		
Pt–C1 (Å)	2.488	2.642[a]
Pt–Si	2.622	2.671[a]
Si–C1	2.147	2.088[a]
Si–C2	3.102	3.430[a]
Si–C3	4.293	4.583[a]
TSd		
Pt–C1	2.469[a]	2.673
Pt–Si	2.475[a]	2.559
Si–C1	2.126[a]	2.059
Si–C2	3.113[a]	3.367
Si–C3	4.375[a]	4.549

[a] Bond distances in the fully optimized complexes.

smaller value of θ for the case of **TSa** indicates that the steric repulsion between Pr and $SiPh_3$ is larger than that between Pr and $Pt(PMe_3)$. This relation of steric repulsion is in consistent with the calculated activation energies in Table 2. The substitutions of PhC≡CPh and PMe_3 (**TSb**, **TSc**, and **TSe**) decrease the activation energies of **TSa** in 1.8–4 kcal mol^{-1} (except for **TSe** of R = Pr: 7.9 kcal mol^{-1}). On the other hand, the substitution of $SiPh_3$ (**TSd** and **TSf**) decreases in 6.5 and 8.7 kcal mol^{-1} for R = Me, respectively, while it does in 11.5 and 14.5 kcal mol^{-1} for R = Pr.

Table 2 shows that activation energies are roughly correlated with the transition state geometries. When the activation energy takes a larger value, the Pt–C1 and Pt–Si bonds are elongated and the Si–C1 bond is shortened, indicating that the TS geometry is more product-like. It is interesting that the activation energies for **TSd** and **TSf** with R = Me are similar to those with R = Pr within 2 kcal mol^{-1}. In contrast, a difference in activation energy for **TSa** of Me and Pr is 7 kcal mol^{-1}. If the activation energy is determined only by a R–Si bond energy [5,7], the present results imply that the energy difference between Me–SiH_3 and Pr–SiH_3 should be smaller than that between R–$SiPh_3$ bonds. By optimizing silyl and alkyl radicals, the Me–Si and Pr–Si bond energies of R–SiH_3 (R–$SiPh_3$) were calculated to be 81.6 (80.4) and 77.0 (75.3) kcal mol^{-1}, respectively. The bond energy difference for R–SiH_3 (4.6 kcal mol^{-1}) is very close to that for R–$SiPh_3$ (5.1 kcal mol^{-1}). Therefore it is concluded that the alkyl-group dependence of the activation energy arises from not only the R–Si bond energy difference but also steric repulsion between the ligands. The most reasonable scenario for interpretation would be the following: when ligands in a Pt complex are bulky, transition state geometry becomes more product-like in order to relax the steric repulsion, and energy difference between the Si–alkyl bonds to be formed in the product becomes more appreciable in determining the activation energy.

4. Conclusions

We have studied the C–Si reductive elimination from $Pt(R)(SiPh_3)(PMe_3)_2$ (R = Me, Pr) by the DFT/B3LYP calculation. Both dissociative and associative mechanisms were shown to contribute to the PMe_3–(PhC≡CPh) ligand displacement for the starting complexes. The R dependence of reaction energy was not observed for this step. The activation barrier of the C–Si elimination from $Pt(Pr)(SiPh_3)(PMe_3)$(PhC≡CPh) was calculated to be 28.9 kcal mol^{-1}, which was 6.9 kcal mol^{-1} larger than for R = Me. Calculations for the model complexes indicates that one of the important factors for the energy difference is steric repulsion between the alkyl and silyl groups at transition state geometry. When the alkyl group is bulky, the TS geometry becomes more product-like and the C–Si bond energy to be formed gives additional contribution to reactivity in the reductive elimination.

Acknowledgements

This work was supported by a Grand-in-Aid for Young Scientists (B) to M.S. from the Ministry of Education, Culture, Sports, Science, and Technology, Japan. The authors thank the Research Center for Computational Science, Okazaki National Research Institutes for a grant of CPU time.

References

[1] A.J. Chalk, J.F. Harrod, J. Am. Chem. Soc. 87 (1965) 16.
[2] F. Ozawa, T. Hikida, T. Hayashi, J. Am. Chem. Soc. 116 (1994) 2844.
[3] F. Ozawa, T. Hikida, K. Hasebe, T. Mori, Organometallics 17 (1998) 1018.
[4] S. Sakaki, N. Mizoe, M. Sugimoto, Organometallics 17 (1998) 2510.
[5] K. Hasebe, J. Kamite, T. Mori, H. Katayama, F. Ozawa, Organometallics 19 (2000) 2022.
[6] F. Ozawa, M. Kitaguchi, H. Katayama, Chem. Lett. 28 (1999) 1289.
[7] F. Ozawa, J. Organomet. Chem. 611 (2000) 332.
[8] (a) A.D. Becke, J. Chem. Phys. 98 (1993) 5648;
(b) C. Lee, W. Yang, R.G. Parr, Phys. Rev. B 37 (1988) 785.
[9] (a) P.J. Hay, W.R. Wadt, J. Chem. Phys. 82 (1985) 299;
(b) W.R. Wadt, P.J. Hay, J. Chem. Phys. 82 (1985) 284.
[10] (a) W.J. Hehre, R. Ditchfield, J.A. Pople, J. Chem. Phys. 56 (1972) 2257;
(b) M.M. Francl, W.J. Pietro, W.J. Hehre, J.S. Binkley, M.S. Gordon, D.J. DeFrees, J.A. Pople, J. Chem. Phys. 77 (1982) 3654.
[11] T.H. Dunning, P.J. Hay, in: H.F. Schaefer (Ed.), Methods of Electronic Structure Theory, Plenum Press, New York, 1977, p. 1.
[12] GAUSSIAN 98, Revision A.11.3, M.J. Frisch, G.W. Trucks, H.B. Schlegel, G.E. Scuseria, M.A. Robb, J.R. Cheeseman, V.G. Zakrzewski, J.A. Montgomery, Jr., R.E. Stratmann, J.C. Burant, S. Dapprich, J.M. Millam, A.D. Daniels, K.N. Kudin, M.C. Strain, O. Farkas, J. Tomasi, V. Barone, M. Cossi, R. Cammi, B.

Mennucci, C. Pomelli, C. Adamo, S. Clifford, J. Ochterski, G.A. Petersson, P.Y. Ayala, Q. Cui, K. Morokuma, N. Rega, P. Salvador, J.J. Dannenberg, D.K. Malick, A.D. Rabuck, K. Raghavachari, J.B. Foresman, J. Cioslowski, J.V. Ortiz, A.G. Baboul, B.B. Stefanov, G. Liu, A. Liashenko, P. Piskorz, I. Komaromi, R. Gomperts, R.L. Martin, D.J. Fox, T. Keith, M.A. Al-Laham, C.Y. Peng, A. Nanayakkara, M. Challacombe, P.M.W. Gill, B. Johnson, W. Chen, M.W. Wong, J.L. Andres, C. Gonzalez, M. Head-Gordon, E.S. Replogle, J.A. Pople, Gaussian, Inc., Pittsburgh PA, 2002.

[13] S. Sakaki, N. Mizoe, Y. Musashi, B. Biswas, M. Sugimoto, J. Phys. Chem. A 102 (1998) 8027.